Results from the Helicopter Drop Test of the DAVINCI Descent Sphere

Soumyo Dutta*, N. Giovanny Guecha-Ahumada†
NASA Langley Research Center, Hampton, VA 23681, USA

Matthew J. Andreini†, Christopher D. Karlgaard*
Analytical Mechanics Associates, Hampton, VA 23666, USA

Matthew Chan‡
NASA Langley Research Center, Hampton, VA 23681, USA

This paper summarizes the October 2023 helicopter drop test of the descent sphere of the upcoming Deep Atmosphere Venus Investigation of Noble gases, Chemistry, and Imaging mission to Venus. The drop test met its primary objectives of recording acceleration, attitude rates, and camera data during the 30-second descent at Utah Test and Training Range. The recorded inertial measurement unit and global position sensor receiver data has allowed a six degree-of-freedom reconstruction of the vehicle position, velocity, attitude, and attitude rates, as well as derived aerodynamic coefficients. Initial comparisons show good agreement between the reconstruction and the pre-flight models of the descent sphere being used by the Venus mission. The reconstructed aerodynamic coefficients from the drop test can inform updates to the aerodynamic model to be used for the actual Venus mission.

Nomenclature

C_A	=	axial force coefficient
C_{L_α}	=	lift curve slope
C_N	=	normal force coefficient
C_X, C_Y	=	force coefficient in coordinate axis
C_l	=	rolling moment coefficient
C_m	=	pitching moment coefficient
C_{mq}	=	pitch damping coefficient
C_n	=	yawing moment coefficient
C_{nr}	=	yaw damping coefficient
Fr	=	Froude number
F_k	=	Force by the k-the spin vane
Ixx, Iyy, Izz_{COM}	=	moments of inertia at center of mass
Ixy, Ixz, Iyz_{COM}	=	products of inertia at center of mass
K	=	number of spin vanes
L	=	reference length
M_k	=	Moment by the k-the spin vane
N_L, N_g, N_ρ, N_μ	=	scaling ratio in length, gravity, density, and viscosityF
R	=	radius of the vehicle at max diameter
S_k	=	reference area of the k-th spin vane
$X_{COM}, Y_{COM}, Z_{COM}$	=	center of mass locations
p	=	yawing rate
q	=	pitching rate

*Aerospace Engineer, AIAA Associate Fellow.
†Aerospace Engineer, AIAA Member.
‡NASA OSTEM Intern, AIAA Student Member.

r	=	rolling rate
g	=	gravitation acceleration
V_∞	=	freestream flow velocity
α_k	=	incidence angle of the k-th spin vane
ρ	=	atmospheric density
ρ_∞	=	freestream density
σ	=	standard deviation
μ	=	atmospheric viscosity
ω	=	roll rate

I. Introduction

The Deep Atmosphere Venus Investigation of Noble gases, Chemistry, and Imaging (DAVINCI) mission is scheduled to launch in June 2029 and explore Venus via two flybys and a probe descent currently scheduled for June 2031. DAVINCI is the 16th selection of the NASA Discovery-Class program and its objectives include quantifying the chemical composition of the Venusian atmosphere, taking infrared descent imagery of the surface, and conducting remote observations of the dynamic atmosphere and cloud-deck. The goals are to study the origin, evolution, and current state of Venus, to understand if it was habitable at a point in the past, and to create an analog to hot terrestrial exoplanets similar to Venus [1].

The Entry, Descent, and Landing (EDL) sequence used by the Probe Flight System (PFS) will be a crucial part of the mission, particularly in its delivery of the Descent Sphere (DS) also called Zephyr, which holds the majority of DAVINCI's on-board instruments for in-situ observations (see Fig. 1). The PFS will be released from the Carrier-Relay-Imaging Spacecraft (CRIS) two days before entry interface. The PFS will be spin-stabilized with a 5 rotations per minute (RPM) roll to meet project requirements, will conduct a ballistic entry of the atmosphere, and will then traverse the Venus atmosphere in one hour. All essential on-board science and engineering data will be transmitted to the CRIS before reaching the Venusian surface. Science operations after landing are not part of the baseline mission; however, Zephyr may continue to transmit data after impact.

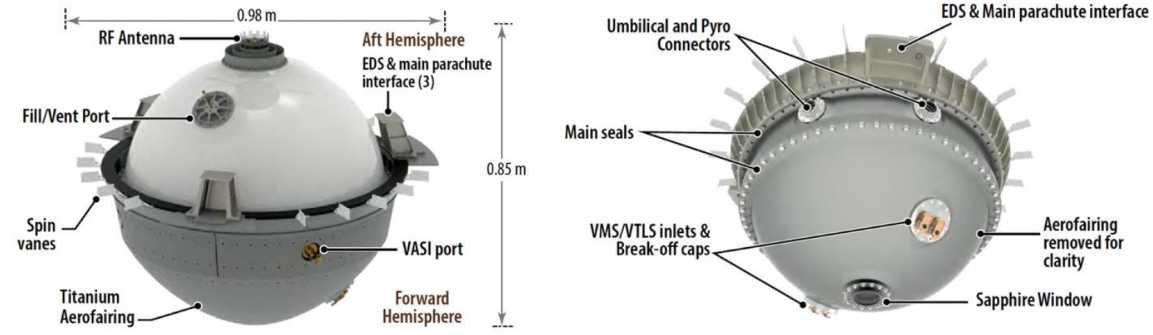

Fig. 1 DAVINCI Descent Sphere - Zephyr [1].

The DAVINCI concept of operations is shown in Fig. 2. The atmospheric interface of the vehicle is modeled at 145 km altitude, and within a couple of minutes, the vehicle undergoes peak heating, peak dynamic pressure, and reaches subsonic conditions. When the vehicle nears 70 km altitude and Mach 0.8, a g-trigger based algorithm triggers a pilot parachute deployment via mortar, and the main parachute is then pulled by the pilot a few seconds later. The heatshield is then jettisoned shortly after allowing the science instruments on the Zephyr to begin their measurements [2]. For the 1-hour EDL portion of the flight, the vast majority of the time is spent with the Zephyr exposed to the atmosphere of Venus. Characterizing the aerodynamics of the vehicle is crucial to predicting the trajectory and performance of the vehicle, as well as ensuring that scientific measurements taken by the instruments on-board Zephyr are collected at desired conditions.

Current aerodynamics models used for the trajectory and performance predictions of Zephyr (see Ref. [2]) are based on historical Pioneer Venus data and engineering results of a Venus descent sphere proposal from the past. However, reconstruction of past planetary descent spheres, such as Huygens, has underscored the importance of developing an aerodynamic model for the actual vehicle being used in the mission and analyzing the outer mold line (OML) of the

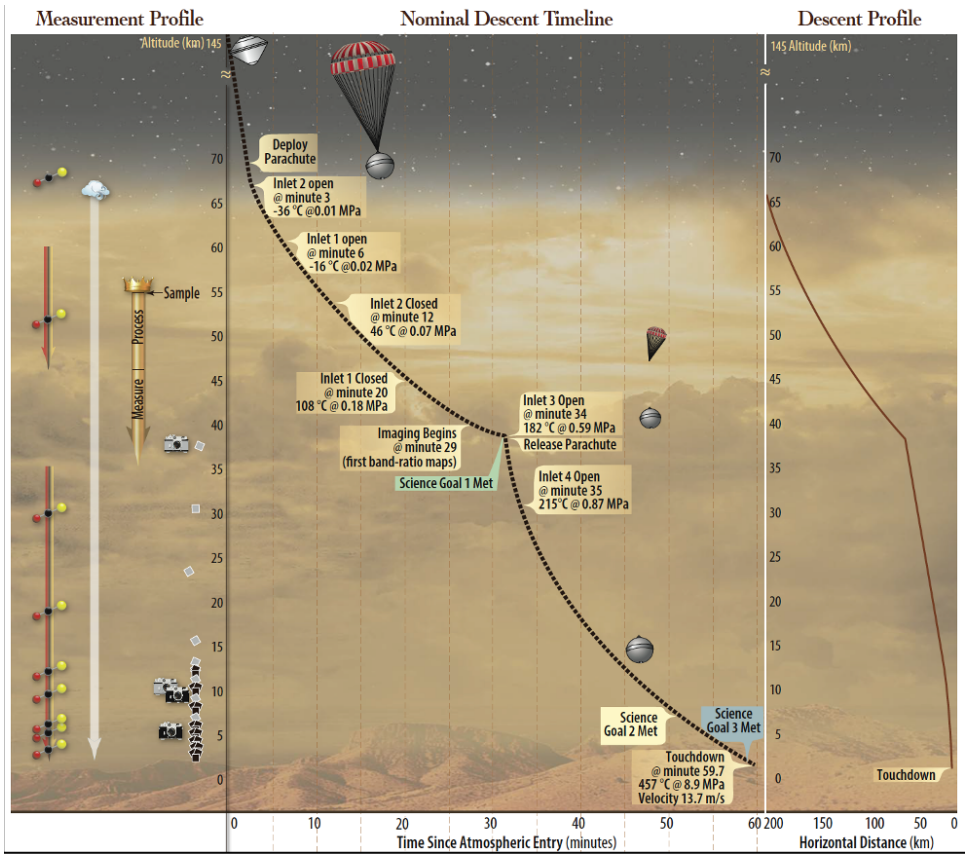

Fig. 2 DAVINCI EDL concept of operations [3].

vehicle [4, 5]. For example, Huygens had a rotational rate in the opposite direction than desired due to an addition to the OML that was not analyzed pre-flight [4, 5]. Hence, an aerodynamic test program using various test facilities, such as free-flight wind tunnels, free-flight drops from drones and helicopters, captive wind tunnel tests, and water tests, were considered to characterize the Zephyr aerodynamics [6].

The focus of this paper will look at the planning and test results of a helicopter drop test of Zephyr test unit that was conducted in October 2023. The objective of the test was to acquire free-fall acceleration and attitude rate data as a proof-of-concept for any potential future drop tests. However, the data collected could be used to characterize aerodynamic properties of Zephyr in a narrow set of Venus-relevant altitude. The test was modeled on past Pioneer Venus drop tests from the 1970's [7].

II. Drop Test Plan and Article

The test was executed in coordination with the Mars Sample Return (MSR) Earth Entry System (EES) project for their high altitude drop test campaign [8]. The EES team provided testing support for a single high altitude drop of the Zephyr Test Unit (ZTU) provided by the DAVINCI project. The test was designed as a proof-of-concept for the instrumentation and test unit to inform the design of potential future drop tests for the DAVINCI mission. The high altitude drop test campaign was conducted at the Utah Test and Training Range (UTTR) in October 2023. The drop test location is shown in Fig. 3. The test would affect a very small area of the range and was a low impact event.

The primary test objective consisted of collecting the acceleration and attitude rates during descent using the on-board inertial measurement unit (IMU). Three secondary test objectives included capturing position and velocity data using on-board global position system (GPS) receivers. Additionally, acquiring high-rate acceleration data during impact to inform the structural design for future tests; and lastly capturing still-frame photos during descent using a nadir-pointing camera. Additional data included video acquired from situational awareness cameras placed on the drag plates and at the helicopter hook. The instruments can be seen in Fig. 4.

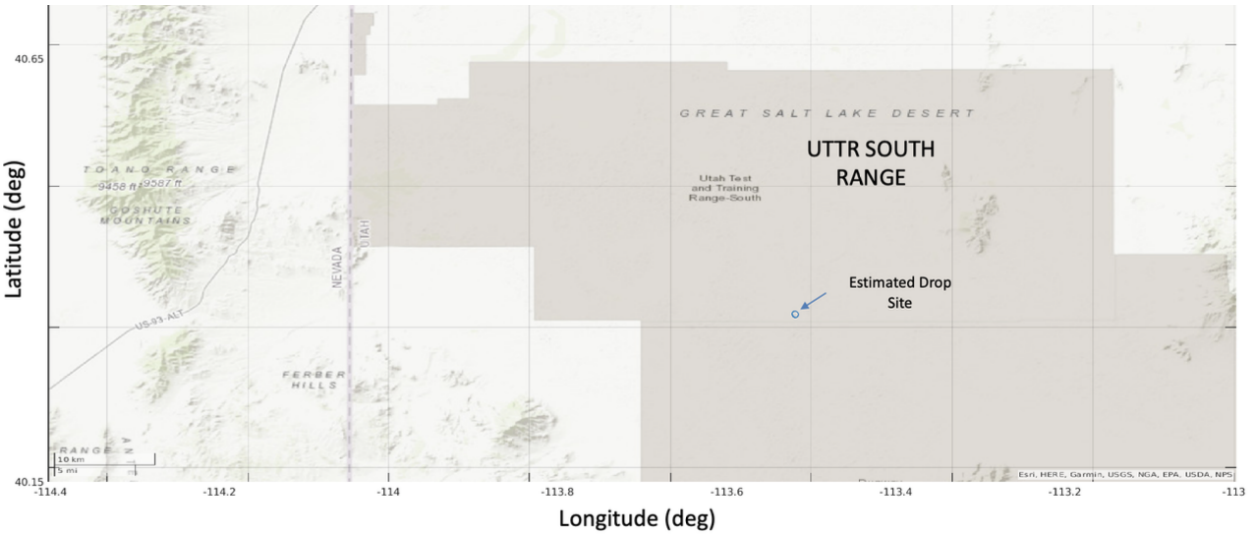

Fig. 3 DAVINCI Zephyr UTTR Drop Test Location.

(a) Casing for cameras (b) DTS IMU (c) Helicopter hook, GPS Watch, and FlySight GPS and IMU

Fig. 4 Zephyr UTTR test model instrumentation.

The ZTU instrumentation suite included accelerometers and rate sensors (contained in the Inertial Measurement Units, IMU), GPS receivers, and visible cameras. These instruments were intended to capture the 6-degree-of-freedom position, velocity, attitude, and attitude rates of the ZTU during freefall along with high-rate accelerometer data to inform aerodynamic and structural reconstruction. The instrumentation suite is summarized in Table 1. The Diversified Technical Systems (DTS) IMU acquired data at 500 Hz and was mounted near the center of gravity of the vehicle (see Fig. 4(b)). The FlySight GPS sensor was mounted on top of the ZTU (see Fig. 4(c)). The FlySight unit also included a miniature IMU that recorded data at 13 Hz. The DTS IMU was the primary sensor for flight reconstruction, however the FlySight IMU data was also analyzed for completion.

Capturing the acceleration and attitude rates of the vehicle would allow the reconstruction of the forces and moments acting on the vehicle, and consequently the aerodynamic forces and moment coefficients. The rolling moment due to the spin vane geometry and incidence angle was of particular interest to validate preliminary roll rate models with flight data. The nadir-pointing camera was set to capture still frame pictures during descent to support the algorithm development of the Venus Descent Imager (VenDI) instrument which will be contained in the Zephyr Venus probe [1]. The still frame pictures were used to reconstruct the terrain with a process analogous to that which will be used by VenDI during the DAVINCI mission. The process and the results of the imaging experiment are summarized in Ref. [9].

The Zephyr Test Unit consisted of a 1.6 scale model dynamically scaled to represent flight conditions at an altitude

Table 1 Instrumentation summary for the Zephyr UTTR test model.

Instrument	Description
GPS	FlySight GPS Sensor/Recorder
GPS	Garmin Watch
IMU	FlySight IMU Sensor/Recorder
IMU	DTS 6-DOF Low-G Acceleration/Rate Sensor
Camera	3x Sony Camera Situational (on drag plates)
Camera	GoPro HERO10 Black Real-Time camera (nadir pointing)
Camera	Sony Camera Situational (on helicopter hook)

of 30 km above the surface of Venus (near parachute release). The model mass properties were related to the Venus flight probe using Froude scaling, which is appropriate for flight testing in which both aerodynamic and gravity forces are important (valid for incompressible flow). The Froude number (Fr) is a non-dimensional parameter defined as the ratio of flow speed (V_∞) to the external gravity (g) field as shown in Eq. 1 where L is the reference length.

$$Fr = \frac{V_\infty}{\sqrt{gL}} \tag{1}$$

The scaling ratio (N) is defined as the ratio of the model value to full-scale value, for instance the length scale N_L for the test was 1.6. The scaling ratios for gravitational acceleration (N_g), and atmospheric density (N_ρ), and viscosity (N_μ) were calculated assuming an altitude of 30 km above Venus for the full-scale values and an altitude of 1.6 km above the Earth mean sea level (mean altitude at UTTR) for the model parameters. Froude scaling parameters are summarized on Table 2. The equivalent mass and mass moments of inertia of the test article were defined using the Froude scaling factors as a function of N_L and N_ρ. The mass properties of the full-scale vehicle and model are summarized in Table 3; however, the mass properties and reference diameter of the full-scale Zephyr probe have changed since the drop test.

Table 2 Froude Number scaling parameters for the UTTR test article.

Parameter	Earth Model (0 km Earth Above Ground Level)	Venus Equivalent (30 km Venus Altitude)
Scale	N_L = 1.6	1.0
Gravitation Acceleration	9.807 m/s^2	8.870 m/s^2
		N_g = 1.106
Atmospheric Density	1.225 kg/m^3	10.15 kg/m^3
		N_ρ = 0.1207
Atmospheric Viscosity	1.789x10^{-5} N*s/m^2	2.36x10^{-5} N*s/m^2
		N_μ = 0.758

The ZTU was constructed from two spun aluminum hemispherical shells. The two hemispheres were attached and reinforced with a steel belt placed at the equator. The most important aerodynamic appendages, the drag plates (horizontal plates) and spin vanes (vertical fins), were additively manufactured (3D printed) using polycarbonate and were attached to a support ring held by the steel belt. The upper hemisphere of the ZTU had a cutoff to allow the inclusion and removal of onboard instrumentation and ballast mass. Pictures of the ZTU during different stages of the test are shown in Fig. 5. The coordinate system used for the Zephyr test article is shown in Fig. 6, where p, q, and r are the rotation rates in the vehicle X, Y, and Z coordinate directions.

This experiment was the first helicopter drop test of a spherical probe shape for Venus since the Pioneer Venus era (Ref. [7]. Similarly to drop tests of that time, the model diameter was greater than its full-scale counterpart to improve the Reynolds number similarity. Matching the Reynolds numbers expected at low Venus' altitudes is particularly challenging due to the dense nature of the atmosphere.

In 2023 and early 2024, the DAVINCI project also conducted three wind tunnel tests at NASA Langley's 20-ft Vertical Spin Tunnel (VST) and one test in the 12-ft Low Speed Tunnel facilities to characterize the aerodynamics of the

Table 3 Mass properties of full-scale and test model.

Parameter	Full-Scale Zephyr (2023 Version)	Drop Test Model (30 km Venus Altitude)
Scale	100%	160%
Reference diameter (drag skirt)	0.87 m	1.392 m
Reference area	0.594 m^2	1.522 m^2
X_{COM}	0.47 mm	-2 mm
Y_{COM}	-0.75 mm	4 mm
Z_{COM}	51.4 mm	154 mm
Mass	285 kg	127.9 kg
Ixx_{COM}	17.60 kg-m^2	26.773 kg-m^2
Iyy_{COM}	17.59 kg-m^2	26.958 kg-m^2
Izz_{COM}	20.53 kg-m^2	29.793 kg-m^2
Ixy_{COM}	0.011 kg-m^2	-0.113 kg-m^2
Ixz_{COM}	-0.1092 kg-m^2	-0.118 kg-m^2
Iyz_{COM}	0.0643 kg-m^2	0.253 kg-m^2

(a) Pre-flight (b) Under Helicopter (c) Post Touchdown

Fig. 5 Zephyr UTTR test model in different stages of development and testing.

vehicle. The VST tests were in free-flight mode, where the vehicle was released in a vertical channel of flow, while the 12-ft test was a captive test with the model mounted on a sting. While the wind tunnel tests provide valuable force and moment information, the flow conditions are limited by facility limits, and are not close to the Reynolds number and Mach number expected for the flight at Venus (see Fig. 7) while the Zephyr is under the parachute or in free fall. The UTTR helicopter drop test did not capture the full gamut of the Venus flow conditions, but does provide test data over a larger range of flow conditions than the wind tunnel tests.

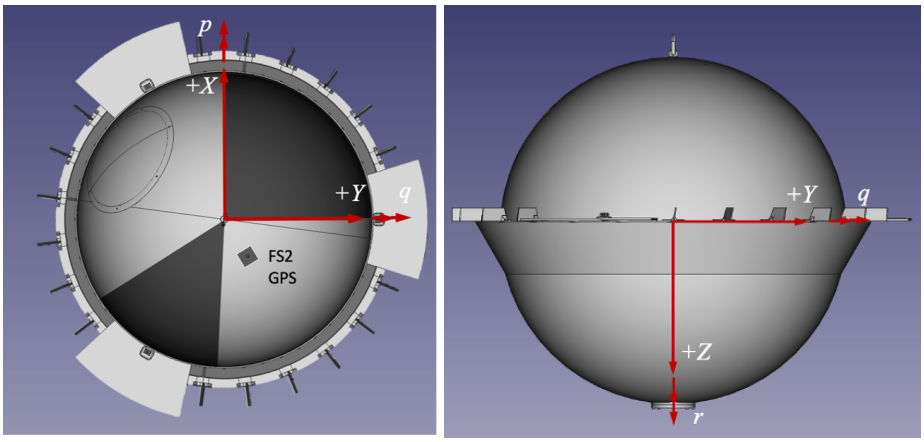

(a) Top View (b) Side View

Fig. 6 Zephyr UTTR test model coordinate system.

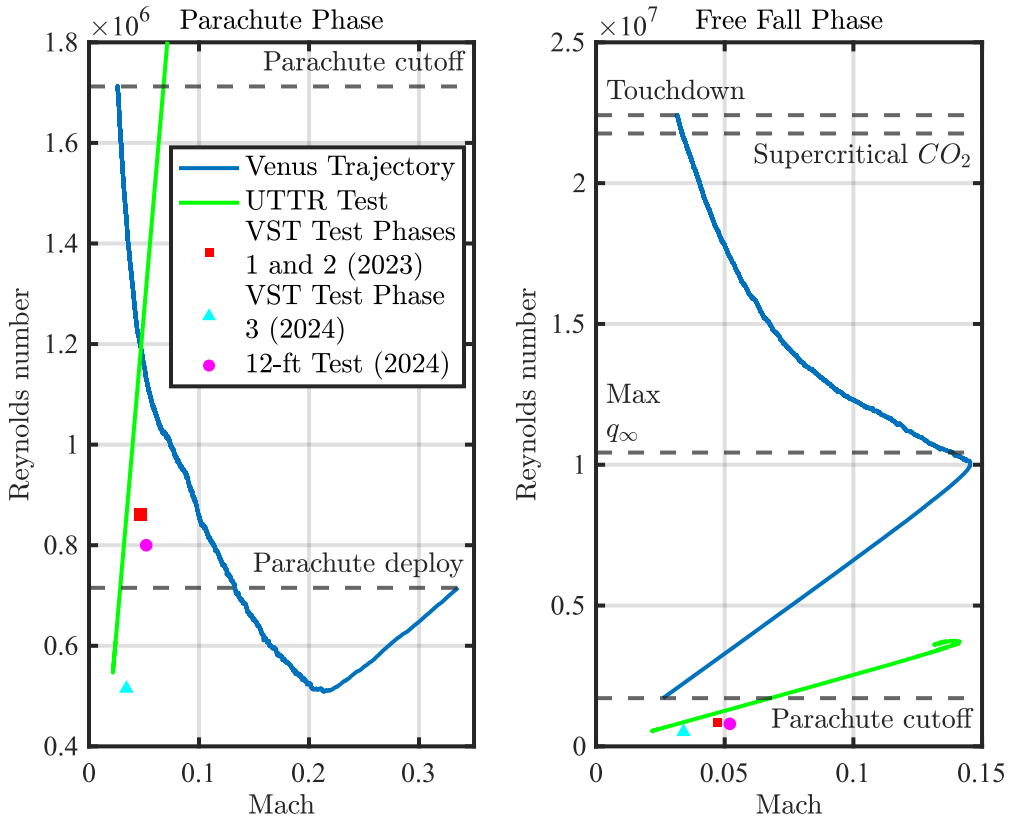

Fig. 7 Flow conditions of the DAVINCI flight at Venus and comparison to conditions of Earth-based tests.

III. Aerodynamic Modeling

The aerodynamic models used for the UTTR model pre-flight simulation were equivalent to those used for the Zephyr Venus descent probe, except for the aerodynamic roll moment model. The current Zephyr aerodynamics model is based on Pioneer Venus Large Probe (PVLP) data [10] and the Venus VISAx proposal from 2010.

The static aerodynamic coefficients were linearized from PVLP wind tunnel test data. The resulting axial force

coefficient model is quadratic with respect to the total angle of attack, whereas the normal force and pitching moment coefficients were linear (constant slope) with respect to the total angle of attack. The aerodynamics are assumed axisymmetric, which implies that the normal force and pitching moment coefficients pass through the origin at a total angle of attack of zero degrees.

The dynamic aerodynamic coefficients, pitch and yaw damping (C_{mq} and C_{nr} respectively), are equal to each other consistent with an axisymmetric assumption and take a constant negative value (dynamically stable). The roll moment aerodynamic components, both static and dynamic, have a value of zero for the Zephyr probe, which follows the assumption that the spin vanes are always oriented parallel to the airflow (spin vanes have an incidence angle of zero degrees), and thus cannot generate a torque (about the probe center of gravity). The spin vanes used for the Zephyr Test Unit were oriented at a non-zero-degree angle to induce a spin rate with the goal of validating new aerodynamic models. An one degree of freedom rolling moment coefficient model for the UTTR test was derived from Huygens post-flight reports (Refs. [4] and [5] with minor changes in nomenclature and corrections) and is described below.

The spin vanes are attached on a ring at the perimeter of the Zephyr as illustrated in Fig. 8. The freestream velocity (V_∞) and the incidence angle (α_k) of the k-th spin vane. The incidence angle of the k-th spin vane and the freestream velocity (measured at the probe center of gravity) is constant; however, the angle between the rotating vane and the airflow experienced by the spin vane is different from α_k and is a function of the angular velocity ω. The orientation of the flow to the spin vane is shown in Fig. 9.

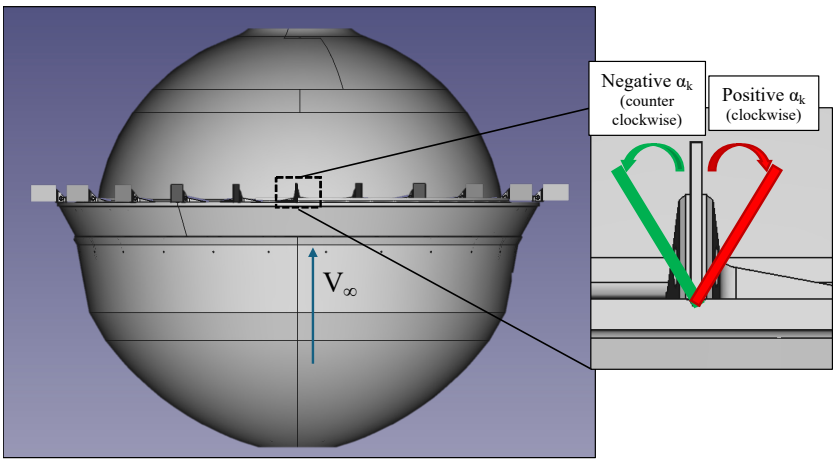

Fig. 8 Orientation and location of the spin vanes on the Zephyr.

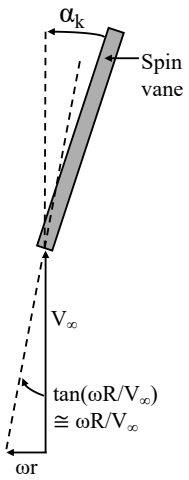

Fig. 9 Spin vane flow angles.

Assuming thin airfoil theory, the k-th spin vane produces a force, F_k (Eqs. 2-3) that depends on the dynamic pressure, the angle between the rotating spin vane and the airflow, and the lift curve slope (C_{L_α}) multiplied by the area of the k-th spin vane (S_k). The equation can be further simplified assuming small angle approximation as shown in Eq. 3.

At the same time, F_k generates a torque (M_k) about the center of gravity of the probe, which is at a distance R from the k-th spin vane (Eq. 4). If the roll moment of inertia (I_{zz}) is given, the sum of moments generated by all spin vanes (K) can be added up to calculate the angular acceleration of the probe (Eq. 5). This ordinary differential equation can be solved numerically to compute the roll rate time history during descent.

$$F_k = \frac{1}{2}\rho_\infty V_\infty^2 \left(\alpha_k - tan(\frac{\omega R}{V_\infty})\right)(C_{L_\alpha} S_k) \tag{2}$$

$$\approx \frac{1}{2}\rho_\infty V_\infty^2 \left(\alpha_k - \frac{\omega R}{V_\infty}\right)(C_{L_\alpha} S_k) \tag{3}$$

$$M_k = F_k R \tag{4}$$

$$I_{zz}\frac{d\omega}{dt} = \sum_{k=1}^{K} M_k \tag{5}$$

Note that this roll rate model assumes that the static and dynamic aerodynamic roll moment coefficients are equal. Moreover, the probe does not contribute to the roll moment. The parameters used to model the roll rate of the Zephyr Test Unit for a simulated descent at UTTR are summarized in Table 4. The ZTU had 18 spin vanes organized in groups of six between the three drag plates. The lift curve slope was the value recommended by Ref. [5], although various lift curve slopes were investigated.

Table 4 Parameter settings for the rolling moment model.

Parameter	Value
α_k	11.0 deg
R	0.696 m
C_{L_α}	2π/5 1/rad
K	18
Chord	47.4 mm
Span	84.3 mm
S_k	3995.8 mm^2

For all of the aerodynamic coefficients, the reference area was based on the drag skirt diameter, which is listed in Table 3, and the drag skirt diameter was used for the reference length. The moment reference point was the centroid of the Zephyr, which coincides with the origin of the coordinate system shown in Fig. 6.

IV. Test Data and Reconstruction

A. Reconstruction Process

The test was successfully conducted on October 3, 2023. The final dataset included two sets of IMU data, two sets of GPS data, weather balloon data, and camera data from all four cameras, the models of which were noted in Table 1. In addition to the weather balloon data, atmospheric information from the reanalysis of a weather forecast model, the Goddard Earth Observing System Model Version 5 (GEOS-5) created by the Global Modeling and Assimilation Office (GMAO) tool at Goddard Space Flight Center (GSFC), was used to provide temperature, pressure, density, and wind information [11, 12].

The reconstruction tool was the New Statistical Estimation Tool (NewSTEP), which has been successfully used for other Earth-based applications [13, 14]. The specific process of reconstructing aerodynamic coefficients given IMU data is identical to NewSTEP's usage for the Mars 2020 reconstruction [15], and explained in detail in Refs. [15] and [16]. NewSTEP uses an iterative Extended Kalman Filter (EKF), where the IMU data is used in the process equations and additional data, such as GPS, are used as observations. Aerodynamic coefficients, such as axial force coefficient (C_A),

normal force coefficient (C_N), pitching moment coefficient (C_m), and rolling moment coefficient (C_l), are processed from the reconstructed trajectory. Additionally, since the EKF is a stochastic filter, the estimated states are characterized as a Gaussian distribution with both the mean and the standard deviation estimated.

B. UTTR Drop Test Simulation

The UTTR drop test was modeled pre-flight to provide predictions for the test. The simulation was modeled in the Program to Optimize Simulated Trajectories II (POST2) tool [17], using the atmospheric model from Earth Generalized Reference Atmosphere Model (GRAM) [18], the aerodynamic model described in Sec. III, and the mass properties from Table 3. The UTTR simulation shares the aerodynamics models with the the Entry and Descent simulation of the DAVINCI also modeled in POST2 (see Ref. [2]). The goal of the UTTR drop test simulation is to utilize DAVINCI Venus simulation's models, especially the aerodynamics modeling, to predict and reconcile with the helicopter drop test data.

Monte Carlo analysis was also conducted with the simulated trajectory to provide statistical predictions of performance based on a 8000-case sample size. An example of the results from the simulation include the landing location in Fig. 3 as well as some of the comparisons of relevant flight parameters, such as position, velocity, attitude, etc., with flight data in the next section.

C. Comparison of the results with simulation

The reconstructed position, velocity, dynamic pressure, and touchdown time, along with comparison to the pre-flight nominal simulation are shown in Figs. 10 and 11. The nominal position and velocity from the pre-flight estimates are close to the reconstructed trajectory and the GPS flight data, especially the estimate of the terminal velocity.

The dynamic pressure comparison shows that despite the differences in the atmospheric models used in the simulation and the experienced aerodynamics in the real flight, the dynamic pressure estimate was close. As mentioned before, the atmosphere in the reconstruction was based on weather balloon data and the GEOS-5 reanalysis data, while the simulation used the Earth GRAM model. Note, the small divergence between the simulation and the reconstruction around 25-30 s right before impact might be atmospheric differences, such as a gust of wind, that is unmodeled in the simulation. Due to the similarity of the reconstruction with the nominal, unsurprisingly the touchdown time is close to one standard deviation (1σ) or Gaussian quantile of the pre-flight, 8000-case Monte Carlo based predictions, as seen in Fig. 11.

The close agreement in position, velocity, and touchdown time suggests a good agreement between the pre-flight and reconstructed force coefficients that govern three-degree-of-freedom type of quantities, such as position and velocity. The reconstructed axial and normal force coefficients are shown in Fig 12, along with the estimate based on the pre-flight model, which used the reconstructed total angle of attack as an input. The figures also show the $\pm 3\sigma$ estimates of the reconstructed force coefficients. The pre-flight axial force coefficient models based on varying angle of attack or the constant value term (which are described in Sec. III) are close to the mean of the reconstructed data, which is also corroborated by the total descent time being similar (Fig. 11). However, it should be noted that the estimated force coefficient's uncertainties are large and the pre-flight model is well within the bounds. For normal force coefficient, the pre-flight model's estimate is compared with the force coefficient estimated in the X and Y axis of the vehicle, as defined by the coordinate system in Fig. 6. The normal force coefficient is an underestimate if compared to the magnitude of either of the reconstructed force coefficients, but is close to the average of the two values.

The reconstructed pitching and yawing moment coefficients are shown in Fig. 13. The pre-flight model (from Ref. [2]) does not differentiate between between pitching and yawing moment coefficients and here the data appear to more closely match the reconstructed yawing moment coefficient. The reconstructed pitching moment coefficient is more stable (less negative) than the pre-flight model. For an axisymmetric vehicle like the Zephyr, pitching and yawing moments should be similar. However, this difference between the pre-flight model and the pitching moment coefficient could be due to uncertainties in mass properties used for reconstruction or other differences.

One of the secondary goals of the UTTR test was to observe the effect of the spin vane incidence angle, α_k, on the rolling rate of the vehicle. For DAVINCI, the vehicle will need to maintain a prescribed roll rate for science operations and stability of the vehicle, and setting spin vane angles to a non-zero α_k is the design variable that can be used to achieve a desired roll rate. The UTTR test article had a α_k of 11 deg, much higher than Pioneer Venus (2 deg) [10] or what DAVINCI would possibly use, to easily observe the rolling motion and increase the signal-to-noise ratio for a short duration drop test. The roll rate from the reconstruction and the simulation can be seen in Fig. 14. Note that in the simulation, the vehicle starts from a zero roll rate, but in flight, the vehicle had some residual spin rate under the

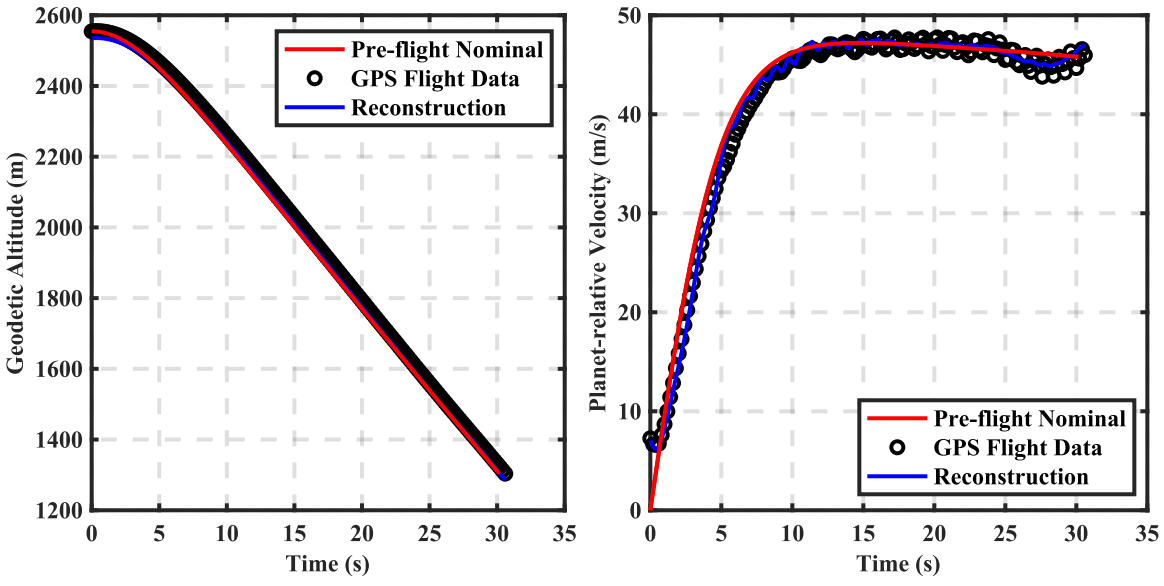

(a) Altitude

(b) Velocity

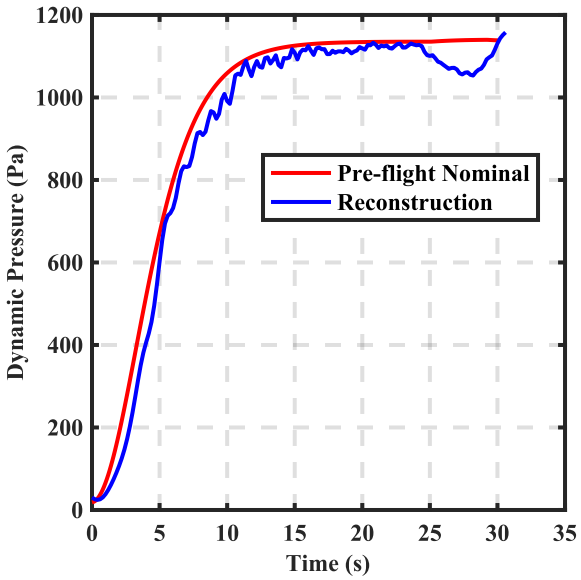

(c) Dynamic Pressure

Fig. 10 Zephyr UTTR test trajectory reconstruction.

helicopter.

In Sec. III, C_{L_α} of the spin vanes was introduced as one of the variables for the rolling moment model. The C_{L_α} used in the simulation is $\frac{2\pi}{5}$ 1/rad or 0.02 1/deg, which is the value from thin airfoil theorem value [5]. However, a few smaller decrements are presented in the figure based on the recommendations in Refs. [4] and [5]. The best fit value appears to be 0.02 1/deg, although the model does not capture some type of damping seen in the reconstructed data.

The rolling moment coefficient from the pre-flight model is assumed to be zero, but a rolling moment model based on thin airfoil theorem and the spin vane incidence angle was developed and presented in Eqs. 2- 5. Due to the existence of spin vanes at a non-zero incidence angle, a non-zero rolling moment coefficient is observed in Fig. 15. The rolling moment from Eq. 4 is non-dimensionalized by the reference length and area based on the drag plate skirt, similar to what was done for the force and other moment coefficients.

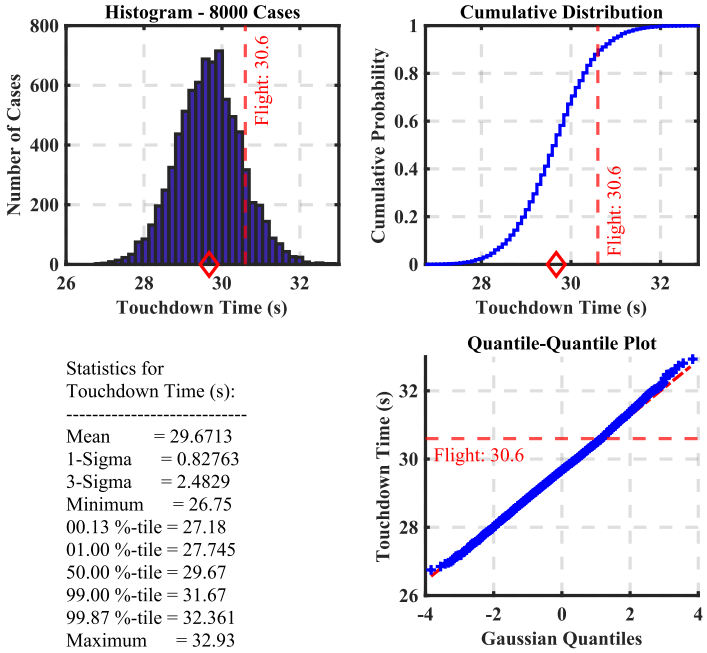

Fig. 11 Zephyr UTTR test trajectory touchdown time.

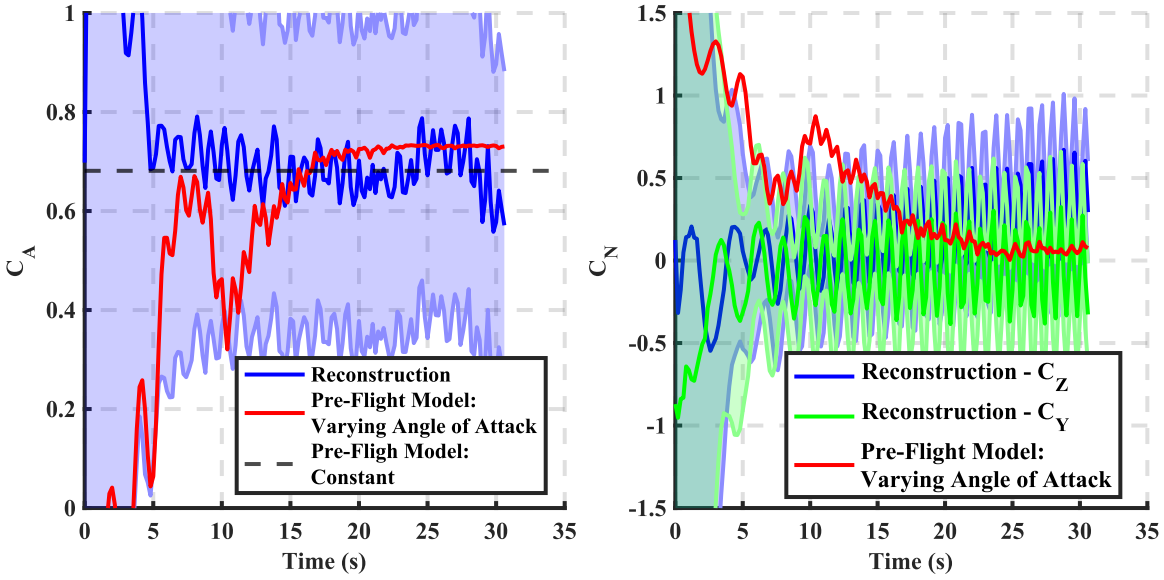

(a) Axial Force Coefficient

(b) Normal Force Coefficient

Fig. 12 Zephyr UTTR test force coefficient reconstruction. The envelopes of the reconstructed quantities signify $\pm 3\sigma$ estimates.

The reconstructed rolling moment coefficient appears to be three to four times larger than the simulation rolling moment coefficient and the reconstruction also shows a gradual damping that is stronger than the current model. Thus, some adjustment to the model derived in Eqs. 2- 5 might be necessary. Nevertheless, the close agreement in the roll rate achieved in the simulation and the actual reconstruction in Fig. 14 shows promise for the existing model.

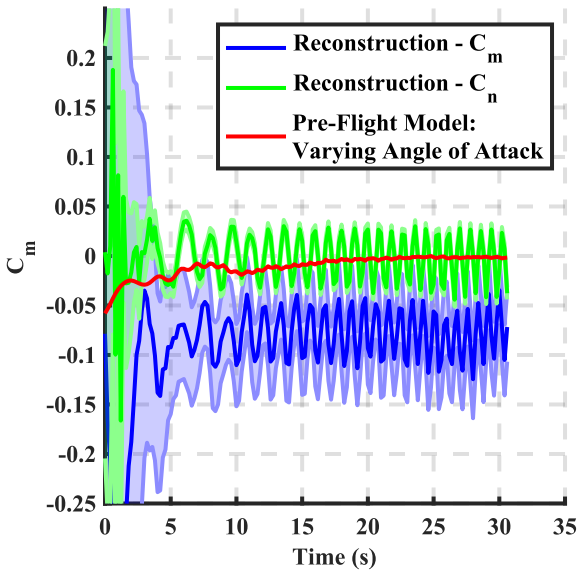

Fig. 13 Zephyr UTTR test pitching and yawing moment coefficient reconstruction. The envelopes of the reconstructed quantities signify $\pm 3\sigma$ estimates.

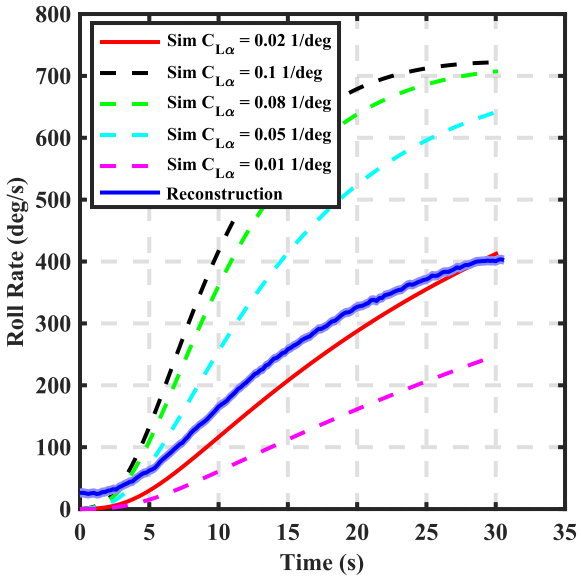

Fig. 14 Zephyr UTTR test rolling rate. The envelopes of the reconstructed quantities signify $\pm 3\sigma$ estimates.

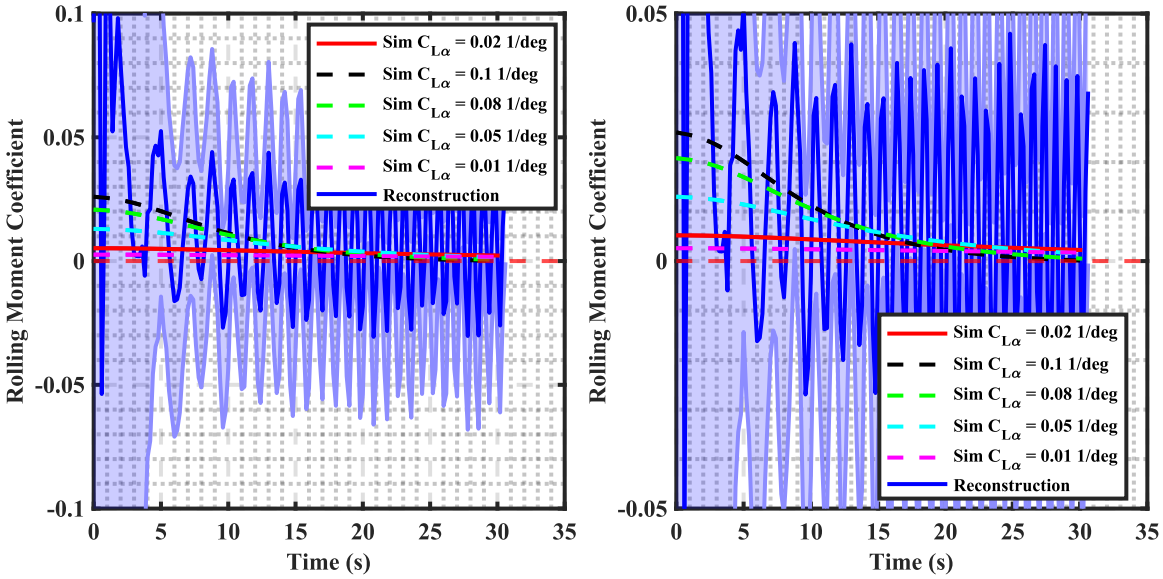

(a) Rolling Moment Coefficient

(b) Zoomed C_l

Fig. 15 Zephyr UTTR test rolling moment coefficient reconstruction. The envelopes of the reconstructed quantities signify $\pm 3\sigma$ estimates.

V. Conclusions

A helicopter drop test was conducted at the Utah Test and Training Range in October 2023 to characterize the performance of the DAVINCI Zephyr descent sphere. The primary test objectives of capturing acceleration, attitude rate, and camera data were met. Additionally, test data from on-board inertial measurement units and global positioning system receivers have been have been used with an iterative Extended Kalman Filter to create a reconstruction of the flight trajectory. The reconstructed trajectory shows good agreement with the pre-flight estimates, especially the rolling rate, and the reconstructed aerodynamic coefficients could be potentially used to update the aerodynamic model of the DAVINCI Zephyr descent sphere.

Acknowledgments

The authors thank the Earth Entry Systems (EES) project and the Langley team who helped facilitate the drop test at UTTR for the DAVINCI Zephyr Test Unit. Special acknowledgements go to Jim Corliss, Eli Shellabarger, Mark Schoenenberger, Jamie Shiflett, and Justin Littell for their guidance in design, execution, and imaging of the testing. Additionally, the authors acknowledge the help of Anthony Williams with some graphics.

References

[1] Garvin, J. B., Getty, S. A., Arney, G. N., Johnson, N. M., Kohler, E., Schwer, K. O., Sekerak, M., Bartels, A., Saylor, R. S., Elliott, V. E., Goodloe, C. S., Garrison, M. B., Cottini, V., Izenberg, N., Lorenz, R., Malespin, C. A., Ravine, M., Webster, C. R., Atkinson, D. H., Aslam, S., Atreya, S., Bos, B. J., Brinckerhoff, W. B., Campbell, B., Crisp, D., Filiberto, J. R., Forget, F., Gilmore, M., Gorius, N., Grinspoon, D., Hofmann, A. E., Kane, S. R., Kiefer, W., Lebonnois, S., Mahaffy, P. R., Pavlov, A., Trainer, M., Zahnle, K. J., and Zolotov, M., "Revealing the Mysteries of Venus: The DAVINCI Mission," *The Planetary Science Journal*, Vol. 3, No. 5, 2022, pp. 297–304. https://doi.org/10.3847/PSJ/ac63c2.

[2] Dutta, S., Guecha-Ahumada, N., Garrison, M., Hughes, K., and Johnson, M., "DAVINCI Venus Entry, Descent, and Landing Modeling and Simulation," AIAA 2023-1165*, AIAA SciTech 2023, AIAA Atmospheric Flight Mechanics Conference,* National Harbor, MD, 2023.

[3] Sekerak, M., Saylor, R., Goodloe, C., Bartels, A., Tompkins, S., Amato, M., Everett, D., Hur-Diaz, S., Hughes, K., Garrison, M., Sayal, C., Getty, S., Arney, G., Johnson, N., Garvin, J., Wade, D., Sutter, B., Cuddy, C., Linn, T., and McGee, M., "The Deep Atmosphere Venus Investigation of Noble gases, Chemistry and Imaging (DAVINCI) Mission: Flight System Design Technical Overview," *IEEE Aerospace Conference,* Big Sky, MT, 2022.

[4] Lebraton, J.-P., and Leron, A., "Huygens Close-out activities Final Technical Report, Issue 2.1," Tech. rep., European Space Agency, 2020.

[5] Lorenz, R., Lebreton, J.-P., Leroy, A., and Perez-Ayucar, M., "Evolution of the Huygens Probe Spin During Parachute Descent," *Journal of Spacecraft and Rockets*, Vol. 58, No. 3, 2021, pp. 609–618. https://doi.org/10.2514/1.A34818.

[6] Guecha-Ahumada, N., and Dutta, S., "DAVINCI: Aerodynamic Testing of the Venus Descent Sphere. ," *International Planetary Probe Workshop*, 2022.

[7] Seiff, A., DeRose, C., and Muirhead, V., "Unsteady Aerodynamics and Motions of the Pioneer Venus Probes," *Journal of Spacecraft*, Vol. 19, No. 5, 1982, pp. 404–411. https://doi.org/10.2514/3.62277.

[8] Karlgaard, C., Deshmukh, R., Schoenenberger, M., Manwell, M., and Corliss, J., "Mars Sample Return Earth Entry System Helicopter Drop Test Reconstruction," *AIAA Aerodynamics Decelerator Conference,* Las Vegas, NV, 2024.

[9] Garvin, J., Dutta, S., Guecha-Ahumada, N., Andreini, M., Ravine, M., Slayback, D., Dotson, R., Bos, B., Garrison, M., Arney, G., Kohler, E., Johnson, N., Bartels, A., and Getty, S., "Descent Imaging of Topography Experiment from DAVINCI Descent Sphere Aerodynamic Drop Test over Utah Test and Training Range (UTTR): Implications for Venus Tesserae Geology," *The Planetary Science Journal (submitted)*, 2024.

[10] "Pioneer Venus Program – Large & Small Probe Data Book," Contract NAS2-8300, HS507-5164, Hughes Aircraft Company, Space and Communications Group, June 1976.

[11] "MERRA-2 instU_3d_asm_Np: 3d, diurnal, Instantaneous, Pressure-Level, Assimilation, Assimilated Meteorological Fields V5.12.4," Tech. rep., Global Modeling and Assimilation Office (GMAO), Greenbelt, MD, 2015. https://doi.org/10.5067/6EGRBNEBMIYS.

[12] Fujiwara, M., Wright, J. S., Manney, G. L., Gray, L. J., Anstey, J., Birner, T., Davis, S., Gerber, E. P., Harvey, V. L., Hegglin, M. I., Homeyer, C. R., Knox, J., Kruger, K., Lambert, A., Long, C. S., Martineau, P., Molod, A., Monge-Sanz, B. M., Santee, M. L., Tegtmeier, S., Chabrillat, S., Tan, D. G. H., Jackson, D. R., Polavarapu, S., Compo, G. P., Dragani, R., Ebisuzaki, W., Harada, Y., Kobayashi, C., McCarty, W., Onogi, K., Pawson, S., Simmons, A., Wargan, K., Whitaker, J. S., and Zou, C.-Z., "Introduction to the SPARC Reanalysis Intercomparison Project (S-RIP) and overview of the reanalysis systems," *Atmospheric Chemistry and Physics*, 2017, pp. 1417–1452. https://doi.org/10.5194/acp-17-1417-2017.

[13] Dutta, S., Karlgaard, C., Tynis, J., O'Farrell, C., Sonneveldt, B., Queen, E., Bowes, A., Leyleck, E., and Ivanov, M., "Advanced Supersonic Parachute Inflation Research Experiment Preflight Trajectory Modeling and Postflight Reconstruction," *Journal of Spacecraft and Rockets*, Vol. 57, No. 6, 2020, pp. 1387–1407. https://doi.org/10.2514/1.A34706.

[14] Dutta, S., Karlgaard, C., Korzun, A., Green, J., Tynis, J., Williams, J., Yount, B., Cassell, A., and Wercinski, P., "Adaptable Deployable Entry and Placement Technology Sounding Rocket One Modeling and Reconstruction," *Journal of Spacecraft and Rockets*, Vol. 59, No. 1, 2022, pp. 236–259. https://doi.org/10.2514/1.A35090.

[15] Karlgaard, C., Schoenenberger, M., Dutta, S., and Way, D., "Mars Entry, Descent, and Landing Instrumentation 2 Trajectory and Atmosphere Reconstruction," *Journal of Spacecraft and Rockets*, Vol. 60, No. 1, 2023, pp. 199–214. https://doi.org/10.2514/1.A35440.

[16] Karlgaard, C., Blanchard, R., Kirsch, M., Tartabini, P., and Toniolo, M., "Hyper-X Post-Flight Trajectory Reconstruction," *Journal of Spacecraft and Rockets*, Vol. 43, No. 1, 2006, pp. 105–115. https://doi.org/10.2514/1.12733.

[17] Williams, R., Lugo, R., Marsh, S., Hoffman, J., Shidner, J., and Aguirre, J., "Enabling Thread Safety and Parallelism in the Program to Optimize Simulated Trajectories II," AIAA 2023-0148*, AIAA SciTech 2023, Washington, DC*, 2023.

[18] White, P., and Hoffman, J., "Earth Global Reference Atmospheric Model (Earth-GRAM): User Guide," Tech. rep., TM 2021-0022157, 2021.